Photoinduced Shape Conversion and Reconstruction of Silver Nanoprisms

Bin Tang, Shuping Xu, Jing An, Bing Zhao, and Weiqing Xu*

State Key Laboratory of Supramolecular Structure and Materials, Jilin University, Changchun 130012, People's Republic of China

Received: December 5, 2008; Revised Manuscript Received: February 22, 2009

A series of shapes of silver nanoplates were achieved by adjusting the concentration of citrate in the colloid in the photoinduced process. The local surface plasmon resonance (LSPR) of the silver nanoplates could be tuned gradually in a range from 740 to 440 nm. In contrast, the LSPR band can be photomediated again to the long wavelength region within 620−690 nm only by adding more citrate to the colloidal system. The initial silver nanoprisms converted to the discal shape under the light effect. In this conversion, the coupling effect of the plasmon resonance and the light source speeds up the photothermal reaction. Subsequently, the reconstruction of silver nanoprisms from the nanodisks took place in the presence of more citrate through the photoconversion.

1. Introduction

Silver nanoparticles have attracted considerable attention because of promising applications in various fields such as biological catalysis,[1] detection,[2] sterilization,[3] electronics,[4] and optics.[5] Among the properties, local surface plasmon resonance (LSPR) properties of silver nanoparticles are of tremendous importance to the applications in biolabeling,[6] surface enhanced Raman scattering (SERS),[7] surface enhanced fluorescence (SEF),[8] sensing,[9] and fabrications of nanophotonic devices and circuit.[10] LSPR is sensitive to the size and shape of the nanoparticles and as well as their composition, dielectric environment, and interparticle spacing. In particular, size and shape of nanoparticles are more significant in several aspects that determine the LSPR of the metal nanoparticles. It is thus critical for obtaining optimal properties of silver nanomaterials with respect to their applications as nanodevices that there is development of a new pathway to systematically manipulate the size and shape over the different dimensions. Lots of methods have been developed to control silver nanocrystal shapes for optical tuning, including the photoreduction, polyol process, surfactant-assisted reduction, solvothermal synthesis, thermolysis of precursors, and micelles controlling growth, by which one can produce silver nanostructures in various shapes, such as prisms,[11] hexagons,[12] disks,[13] wires,[14] cubes,[15] bipyramids,[16] and tetrahedrons.[17] Development of the synthetic approaches that involve a high degree of control over the nanoparticle morphology is significant for the applications of silver nanoparticles, such as SEF and SERS.

Thermal[13b,18] and photochemical[11,19] strategies are two main typical approaches for preparing the silver nanoparticles in different shapes and sizes. The different factors that influence particle size and shape have been investigated extensively. Chen et al.[13b] prepared the silver nanodisks from truncated triangular silver nanoplates at 40 °C in the presence of hexadecyl trimethyl ammonium bromide (CTAB). Xia et al.[18a] obtained triangular silver nanoplates with sharp corners by refluxing an aqueous dispersion of spherical colloids in the presence of poly(vinyl pyrrolidone) (PVP) and sodium citrate. The natural light was believed to be the essential factor for the generation of triangular seeds, which led to the transformation of spherical colloids into triangular nanoplates at elevated temperatures. Mirkin et al.[11,19b,20] demonstrated the photomediated growth of silver nanoprisms from spherical silver nanoparticles. They illuminated that both the photochemical and the thermal control cooperated for the silver nanocrystal growth. In their papers, the results suggested that the photochemical process was driven by the silver redox cycles, which involved the reduction of silver cations by citrate on the silver particle surface and the oxidative dissolution of small silver particles. Similarly, Wu et al.[21] described a related mechanism of photoconversion of the aqueous citrate stabilized silver nanocrystal seeds to the disk nanoprisms. It involved photo-oxidation of citrate by hot "holes" from the plasmon dephasing on the surface of the nanoparticles, oxidative etching of silver in the presence of O_2, and selective reduction of aqueous silver ions on crystalline disk prisms with a larger photovoltage. Much effort has been put into the shape conversion and the size tuning of silver nanoparticles.

Herein, we present a photoinduced mediating morphology procedure for obtaining a series of shape conversion of silver nanoparticles in one system, in which silver nanoprisms can transform to nanodisks, and subsequently the as-synthesized nanodisks convert to nanoprisms with a certain quantity of citrate being added into the silver colloids. Significantly, the LSPR of silver nanoparticles can be tuned feasibly in a certain range. The LSPR spectra of silver nanoprisms have been recorded. The relationship between the features of LSPR to the shape conversion at different irradiation time has been analyzed in detail. The citrate concentration and light as significant impacting factors were investigated in the process of mediating morphology of silver nanoplates.

2. Experimental Section

2.1. Materials. $AgNO_3$ (99.8%) was obtained from Shanghai Chemical Reagent Co., Ltd. $NaBH_4$ (96.0%) was purchased from Sinopharm Chemical Reagent Co., Ltd. Trisodium citrate (99.0%) was supplied by the Beijing Chemical Reagent Plant. PVP (M_w = 30 000) was obtained from Beijing Dingguo Biotechnology Co., Ltd. All chemicals were used without any further purification. All of the solutions were aqueous solutions.

* Corresponding author. Tel.: +86-431-85159383. Fax: +86-431-85193421. E-mail: xuwq@jlu.edu.cn.

10.1021/jp810711a CCC: $40.75 © 2009 American Chemical Society
Published on Web 04/01/2009

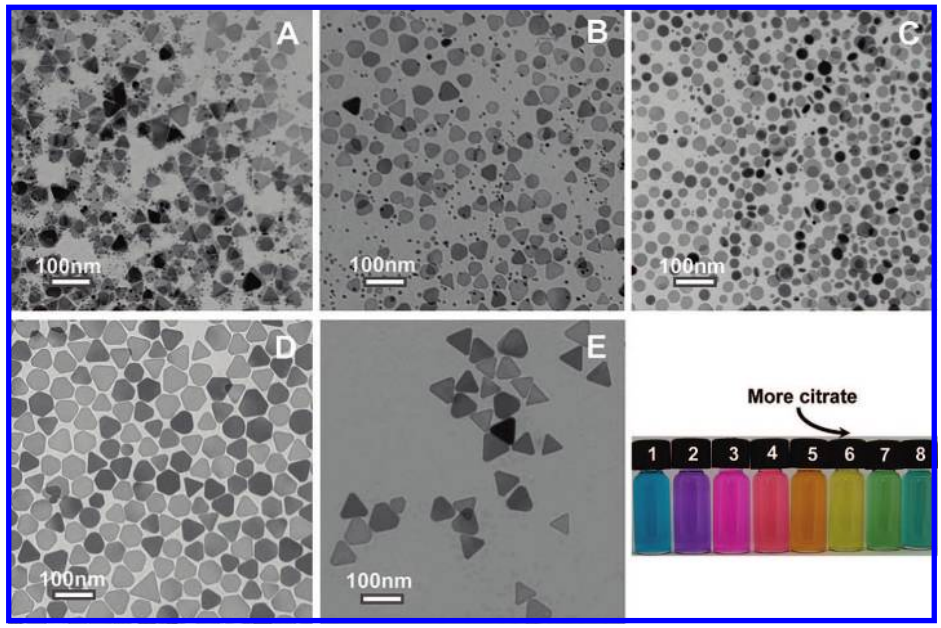

Figure 1. TEM images of (A) initial silver nanoprisms, (B) the intermediate nanoplates in conversion of prisms to disks, (C) nanodisks through photoinduced evolution at the low molar ratio of citrate to Ag, (D) the intermediate nanoplates in conversion of disks to prisms, and (E) final silver nanoprisms evolving from nanodisk colloid after adding more citrate. The lower right panel is the photograph of the silver colloid in the photoconversion process at different irradiation times: (1) 210 min, (2) 330 min, (3) 370 min, (4) 380 min, (5) 390 min, (6) 400 min in the shape conversion, and (7) 530 min, (8) 710 min after adding more citrate into the nanodisk colloid.

The purified water (1.25 L packing) was purchased from Hangzhou Wahaha Group Co., Ltd.

2.2. Shape Evolution of Silver Nanoplates by Photoinducement. A typical experiment was carried out by the photoconversion method.[12b,17,19b] First, silver seeds were prepared by dropwise addition of $NaBH_4$ solution (7.2 mM, 1.0 mL) to an aqueous solution of $AgNO_3$ (0.09 mM, 100 mL) in the presence of trisodium citrate (0.081 mM) under vigorous stirring. Next, the yellow silver seeds (100 mL, in glass conical flask with a cover) were exposed under a sodium lamp (NAV-T 70 model from Osram China Lighting Co., Ltd.). The irradiation power density of the sodium lamp was determined to be 80.6 mW/cm^2 as measured using a Gentec-EO Solo 2 energy and power meter at the position of silver solution. The color of silver colloids changed from yellow, to green, blue, purple, mauve, red, and yellow during the irradiation process. Subsequently, more citrate (81.9 μmol) was added into the yellow silver colloid as-synthesized, and the irradiation continued. In the sequential photoinduced process, the color of the silver colloid changed from yellow, to green, and eventually blue. The ultraviolet−visible (UV−vis) spectroscopy and transmission electron microscope (TEM) were used to monitor the varieties of LSPR spectra and morphologies of the shape evolution. The structure of the crystal facets is discussed in the Supporting Information (Figures S1 and S2).

2.3. Instruments. UV−vis spectra were recorded from by Ocean Optics USB4000 spectrometer. TEM images were measured with a Hitachi H-8100 IV instrument operating at 200 kV. Samples for TEM analysis were prepared by dripping a drop of silver nanoparticle colloids onto the carbon-coated copper grids and drying them in the air at room temperature.

3. Results and Discussion

3.1. Shape Evolution. Figure 1A−E shows the TEM images of the silver nanoplates taken at different representative reaction periods. Figure 1A shows the initial silver nanoprisms, which were fabricated through the photoindcued growth of silver seeds. The mechanism of the photoconversion from silver seeds to nanoprisms has been investigated recently.[20,21] It was suggested that the shape transformation of silver nanoparticles from the spherical (or semispherical) seeds to the prisms is driven by silver redox cycles, which involve both the reduction of silver cations by citrate on the silver particle surface and the oxidative dissolution of small silver particles by oxygen. In this process, a lot of small spherical silver nanoparticles concomitantly appeared with the nanoprisms (Figure 1A) because the citrate was not enough that the silver redox cycles were uncompleted.

The initial as-synthesized nanoprisms can be transformed to the nanodisks as the irradiation reaction continues. Images B and C in Figure 1 show the truncated nanoprisms (an intermediate state) and nanodisks when the silver colloid was exposed to the high pressure sodium lamp for 330 and 400 min. The length of the initial nanoprisms (a_1) is 43.7 ± 4.0 nm. So the diameter of the inscribed circle of the nanoprisms (d_1) is equal to 25.2 nm. The diameter of nanodisks (d_2) is 31.5 ± 3.5 nm, which is 6.3 nm longer than d_1. That means that during the conversion of prisms to disks, the silver atoms simultaneously adsorb on the side {110} facets of nanoplate. The silver atoms at the corner areas have less coordination number of surface atoms than those on the {110} facet, which results in higher surface energy at the corner areas. Therefore, the sides are more stable than the tips, which is in favor of absorption of silver atoms on the sides. In Figure 1B, there were many hexagonal nanoplates that appeared in the colloidal system, which have been reported in our previous work.[12b] In the present study, the nanodisks derived from the nanoprisms are monodisperse and in a high yield (Figure 1C).

Interestingly, by adding more citrate (81.9 μmol) into 100 mL of the as-synthesized nanodisk colloids, the nanodisks under the light irradiation can convert to nanoprisms again. Images C−E in Figure 1 show the shape evolution from the uniform nanodisks to nanoprisms with more citrate. Evidently, the nanoplates underwent other truncated nanoprisms as the intermediate products. Finally, the well-defined nanoplates were

SCHEME 1: Illustration of the Photoconversion of Nanoprism to Nanodisk and Reconstruction of Silver Nanoprism after Adding More Citrate in the Light-Induced Process[a]

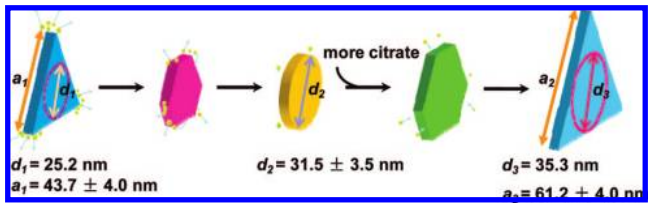

[a] a_1, a_2, and d_2 are measured results; d_1 and d_3 are calculated results.

obtained, and no small nanospheres were observed in the final nanoprism colloids (Figure 1D and E), which indicates that all of the small nanoparticles have been converted to the nanoprisms completely. The edge length of final nanoprisms (a_2) was 61.2 ± 4.0 nm. The process of shape conversion is depicted schematically in Scheme 1. Apparently, the nanoprisms derived from nanodisks are larger than the initial nanoprisms: $a_2 > a_1$ and $d_3 > d_2$ (d_3 as the calculated inscribed circle diameter of the final nanoprism). The enlarged size of nanoprisms proves that all of the small nanoparticles were consumed to make up for the growth of the fresh nanoprisms. This conversion of small silver nanoparticles can be thought of as a light-driven Ostwald ripening process. After more citrate was added into the reaction system, the photo-oxidation of citrate resumed. Moreover, the Ag(I) ions were reduced by the fresh added citrate through the photoinduced process. These nanodisks become the new active sites of Ag(0) growth. The final nanoprisms grew, while the small silver nanoparticles almost disappeared.

3.2. LSPR Evolution. Significant changes in the colors of the silver colloids were observed during the process of shape photoconversion. The blue silver nanoprisms changed to purple, mauve, red, and yellow finally, while the initial prism was transformed to disk. When more citrate was added into the yellow silver colloids and the irradiation of light continued, a series of changes of color occurred again, from yellow to green, and to blue eventually (lower right panel in Figure 1).

Figure 2A and B shows the UV−vis spectral evolution for silver nanoplates before and after more citrate was added. Figure 2C refers to the extinction peak position of Figure 2A versus the irradiation time. Figure 2D shows the plots of the peak position (★) and intensity (▲) of the longest wavelength in Figure 2B versus the irradiation time after addition of more citrate. The conversion process is suggested to include three stages: (I) growth of initial silver nanoprisms; (II) conversion of prisms to disks, at the low concentration of citrate (0.081 mM); and (III) conversion of disks to prisms after 81.9 μmol of citrate was added. We analyzed the peak position at the longest wavelength (λ_{max}) versus the irradiation time in Figure 2C and D. We will discuss in detail the LSPR evolution of these three stages in the next several paragraphs based on Figure 2.

In stage I, four LSPR bands are observed from this spectrum of 210 min (Figure 2A, olive color). Three of them centered at 331, 482, and 661 nm are assigned to the out-of-plane quadrupole, in-plane quadrupole, and in-plane dipole plasmon resonance modes of silver nanoprisms, respectively.[11] The band at 393 nm is attributed to the round silver seeds, which were employed to synthesize the anisotropic nanoparticles through the photoinduced process. The in-plane dipole resonance peak (■ in Figure 2C) first red-shifted and subsequently blue-shifted. We believe it is the process of the fabrication of initial silver nanoprisms that has been illuminated in many reports.[11] This stage may be considered as the incunabulum, in which the silver seeds formed the crystal nanoprisms through the photoconversion involving the oxidation of citrate catalyzed by silver.[20,21]

In the following stage II, the in-plane dipole resonance peak of initial nanoprisms blue-shifted gradually with the irradiation remaining the same (● in Figure 2C). Because the in-plane dipole resonance peak is very sensitive to the size and aspect ratio,[11] the blue-shift of in-plane dipole resonance peak implies that the size and the aspect ratios of nanoplates get reduced. With the light irradiating, the size of nanoplates got smaller and smaller. In stage II, we could find that the trend of λ_{max} has a transition at the time of 360 min. We will discuss this special change on the reaction speed next. In addition, the out-of-plane quadrupole resonance peak red-shifted from 331 to 343 nm. In regard to the spectra at 400 and 410 min, three new LSPR peaks presented at 343, 367, and 443 nm, attributed to the out-of-plane quadrupole, in-plane quadrupole, and in-plane dipole resonant modes of silver nanodisks, respectively.[13a] The intensity of the peak at 393 nm decreased obviously, but it remained unchanged in the spectrum after 400 min, implying a few seeds remained in the final product of the photoinduced growth. That coincides with the results of TEM images (Figure 1C).

As more sodium citrate was added into the colloid of silver nanodisks, the spectral evolution of silver colloid (Figure 2B) shows that a new peak at ~600 nm appeared, which is ascribed to the in-plane dipole resonance mode of silver nanoprisms (★ in Figure 2D). The in-plane dipole resonance peak obtained the maximum (693 nm) at 300 min and then went back slightly after 320 min irradiation. Moreover, as it can be seen from Figure 2D, the intensity increases with the extending of irradiation. That is similar to the seed growth process of initial nanoprisms. The variation of the in-plane dipole resonance peak indicates that the size of nanoplates increases in plane. The out-of-plane quadrupole resonance peak blue-shifted from 343 to 335 nm, which implies that the aspect ratio of nanoplates increases after more citrate is added. The band at about 460 nm contains two resonance modes after more citrate is added: in-plane dipole resonance of nanodisks and the in-plane quadrupole resonance of nanoprisms. With the aspect ratio of nanoplates increasing under the light irradiation, this band gradually separated into two peaks. The extinction peak at ~468 nm, which is assigned to the in-plane dipole resonance mode of nanodisks, remains in the final nanoprisms in stage III. It is due to the incomplete conversion of the nanodisks.

The LSPR of the silver nanoparticles can be tuned facilely by adjusting the irradiation time and concentration of citrate in the reaction system. Interestingly, the effect of light can induce the LSPR band blue-shift steadily, whereas the LSPR band can be photomediated to the long wavelength region only by adding more citrate to the colloidal system.

3.3. Growth Speeding Period from the Coupling of Plasmon Resonance and Irradiation. An emission spectrum of the sodium lamp as light source is shown in Figure S3, which is different from the emission spectra of other typical sodium lamps. According to our observation, the emission spectrum of the lamp lighting up over 20 min is more complicated than that at the beginning. When the lamp has been lit up for a while, the peaks in the visible range increase. Among them, some become broad and overlapped and turn into an emission main band in the range of 560−620 nm in the spectra.

In the growth process of silver nanoparticles by the photo inducement method, we often observe an interesting phenomenon that the growth (denudation or sculpturing) effects of the reaction speed up suddenly. We call it "Growth Speeding Period

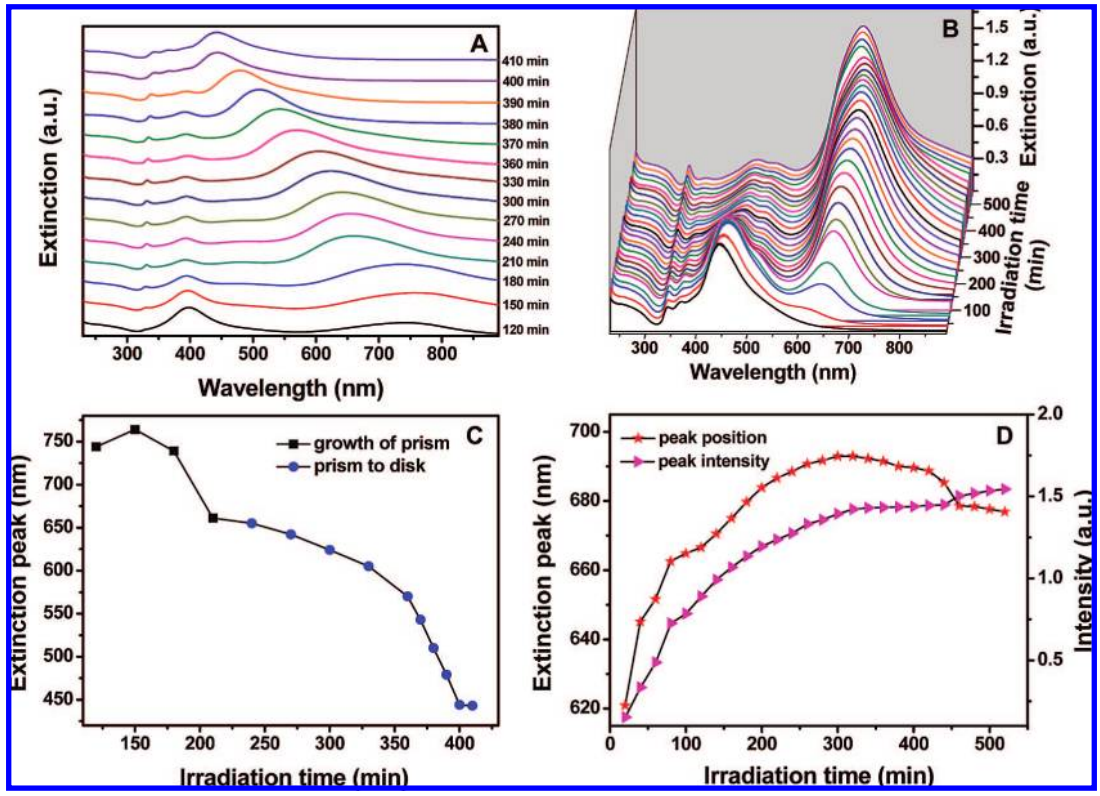

Figure 2. (A) Extinction spectra of silver nanoplates colloid at different irradiation time when the concentration of citrate is 0.081 mM. (B) Extinction spectra of silver nanoplates acquired every 20 min evolving from the as-synthesized nanodisk colloid after 81.9 μmol of citrate was added. (C) Relation of the in-plane dipole resonance peaks in the extinction spectra of (A) versus the irradiation time (initial nanoprisms marked with ■ and nanodisks marked with ●). (D) Plots of the position (★) and intensity (▲) of the in-plane dipole resonance peaks of final nanoprisms in the extinction spectra of (B).

from the Coupling of Plasmon Resonance and Irradiation". It happens when the adjustable plasmon resonance bands overlap the emission band of the irradiation source, and the effect from the light is maximum on the growth of nanoparticles. On the other hand, when the plasmon resonance bands get far away from the emission band of the irradiation source, the light effect decreases. In our present study, stage II gives a coincident example of this phenomenon. In stage I (Figure 2C; 0−210 min), the citrate in the reaction is consumed as the initial nanoprisms grow. The lack of citrate leads to the incomplete conversion of small silver nanospheres in stage I. Moreover, the lack of citrate makes the photochemical effect weaken. When the initial nanoprism growth is almost finished, the in-plane dipole plasmon band of silver nanoprisms at ~661 nm was close to the main emission band of the irradiation source. At this moment, the photothermal effect is enhanced. Therefore, the thermal efficiency of the irradiation source increases. It has been reported that the strongest electromagnetic fields generated by the dipole excitation of triangular nanoprisms are localized at the tips of the nanoprism.[22] So, in this growth speeding period, the tips of the nanoprism grow fast especially. When the overlapping of in-plane dipole band of nanoplates with the main emission band of irradiation source gets to a maximum, the inducement of the irradiation source on the dipole is strongest. Therefore, the photoinduced shape conversion is accelerated. As shown in Figure 2C, the in-plane dipole band blue-shifts mildly in photoinducing time of 210−330 min in the first segment of stage II. However, in the succeeding segment, the blue-shifting accelerates after 330 min, which is attributed to the great photothermal effect derived from the coupling of plasmon resonance and irradiation. When the in-plane dipole band goes away from the irradiation band, the photothermal effect became weak, and blue-shifting of the in-plane dipole band tended to stop. In addition, the power density of irradiating light on the sample solution is 80.6 mW/cm^2, which is high enough that the shape conversion can be achieved including photochemical and photothermal roles.[21] The influence of the power density of light on the photoinduced process has been discussed by us previously.[19e]

3.4. Role of Citrate and Light. The citrate concentration is a pivotal factor influencing the photoinduced evolution. It determines the final morphology of silver nanoparticles and the rate of reaction. It is reported that citrate stabilization is necessary for photoconversion of nanoparticles into prisms.[23] By increasing citrate concentration, the photochemical process can be significantly enhanced as compared to the photothermal process. In stage III, the dipole plasmon excitation by irradiation induces charge separation on the nanodisk surface and assists citrate photo-oxidation on the nanodisk surface.[20,21] A possible anisotropic distribution of charge induced by dipole plasmon excitation results in the shape transformation from the isotropic disks to anisotropic prisms. Both the additional citrate and the light inducement are necessary for conversion of disk to prism.

In the transformation from initial nanoprism to nanodisk, the concentration of citrate in the solution plays a key role. When the concentration of citrate in the solution is more than 0.27 mM, the initial nanoprisms could not transform into the nanodisks through the effect of light, which has been mentioned in a previous report.[12b] The initial nanoprisms convert into the nanodisks if the concentration lies in a range of 0.045−0.20 mM. Figure S4A and B shows the extinction spectra of nanoplates from prism to disk corresponding to the citrate concentrations of 0.045 and 0.20 mM, and the insets are the plots of the in-plane dipole resonance peak and the irradiation

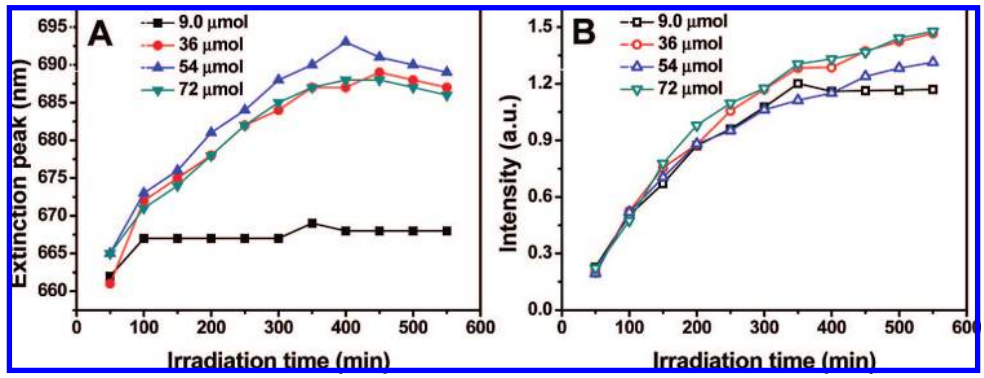

Figure 3. Plots of peak position (A) and intensity (B) at long wavelength of silver colloid with irradiation time after adding different amounts of more citrate with 9.0, 36, 54, and 72 μmol.

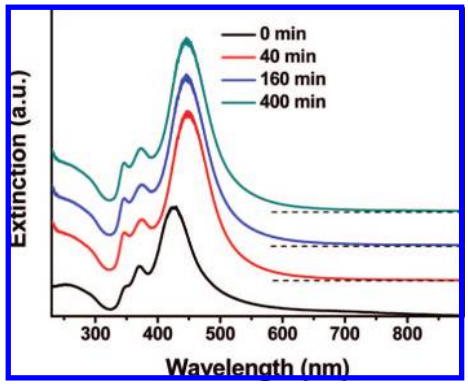

Figure 4. Extinction spectra of silver nanodisk colloid after adding more citrate heated at 90 °C for different times: 0 min, 40 min, 160 min, and 400 min.

time, respectively. As can be seen, the reaction with low concentration of citrate is rapid. When the concentration of citrate is under 0.045 mM, the silver nanoparticles are unstable and easy to aggregate. To gain insight into the influence of the quantity of additional citrate on the reconstruction of nanoprism, different amounts of citrate (9.0, 36, 54, and 72 μmol) were added to silver nanodisk colloid (0.09 M, 100 mL). The respective corresponding spectra are shown in Figure S5. Figure 3A plots the peak position of the in-plane dipole resonance band of nanoplates at different irradiation times when different amounts of citrate were added. The evolutions of λ_{max} are almost consistent except that the evolution of 9.0 μmol changes slower. However, the peak intensities all increased gradually (Figure 3B). So we believe that the shape conversion from disk to prism can be carried out when the amount of citrate is at least 9.0 μmol.

To explore the necessity of citrate in the evolution of disk to prism, PVP was added into the as-synthesized nanodisk colloid instead of the citrate. PVP was usually used to assist the synthesis of silver nanoprisms (for details, see the Supporting Information).[18a,24] The unchanged UV−vis spectra indicated that the PVP could not convert the silver nanodisks to the nanoprisms under the irradiation (Figure S6). It is citrate that has a pivotal role in the transformation from nanodisks to the nanoprisms. Moreover, the produced nanomaterials are stable for a long period, and the citrate as a stabilizer can avoid effectively the aggregation (Figure S7).

In addition to the role of citrate in conversion of disks to prisms, the effect of light is also significant. To clarify the necessity of light in the shape conversion process, irradiation was replaced by heating in treatment of shape evolution from disk to prism. We added more citrate (81.9 μmol) into silver nanodisk colloid (0.09 M, 100 mL) and heated the silver nanodisk colloid at 90 °C in a water bath. The UV−vis spectra of silver nanoparticles red-shifted slightly at the beginning of heating; however, the profile of UV−vis spectra (Figure 4) did not change, and the spectra remained unchanged for a long period of heating (400 min), which indicated that the heating could not facilitate the shape transformation of nanoparticles even though there was enough citrate in the colloidal system.

4. Conclusions

A series of shape conversion from nanoprism, to nanodisk, and to nanoprism in reverse was achieved by controlling the citrate concentration in the system in the light-induced process. The light and the citrate are crucial and irreplaceable for the transformation of silver nanoparticles. The truncation of silver nanoprisms took place, and the rearranging of silver atoms progressed simultaneously under the photothermal control. The coupling effect of the plasmon resonance and the light source speeds up the photothermal reaction. As more citrate was added into the silver nanodisk colloid, the photochemical process was overwhelming and led to the conversion of disks to prisms. The small silver nanospheres and silver cations in the colloidal system were gathered to the disks and formed larger prisms. Remarkably, the LSPR of silver nanoparticles can be tuned flexibly. The silver nanoplates with controllable shape and size, having amusing LSPR optical property, may be applied in potential biological and chemical sensors, as well as in surface enhanced spectroscopy including SERS and SEF.

Acknowledgment. This work is supported by the National Natural Science Foundation of China (NSFC20773045 and 20627002) and the Seed Funding of Jilin University (20805045).

Supporting Information Available: Electron diffraction patterns of individual silver nanoplate, HRTEM images of initial silver nanoprism and nanodisk, and additional extinction spectra. This material is available free of charge via the Internet at http://pubs.acs.org.

References and Notes

(1) (a) Kamat, P. V. *J. Phys. Chem. B* **2002**, *106*, 7729. (b) Pradhan, N.; Pal, A.; Pal, T. *Colloids Surf., A* **2002**, *196*, 247.
(2) Alivisatos, P. *Nat. Biotechnol.* **2004**, *22*, 47.
(3) (a) Jain, P.; Pradeep, T. *Biotechnol. Bioeng.* **2005**, *90*, 59. (b) Pal, S.; Tak, Y. K.; Song, J. M. *Appl. Environ. Microbiol.* **2007**, *73*, 1712.
(4) (a) Li, Y.; Wu, Y.; Ong, B. S. *J. Am. Chem. Soc.* **2005**, *127*, 3266. (b) Lee, K. J.; Jun, B. H.; Kim, T. H.; Joung, J. *Nanotechnology* **2006**, *17*, 2424.
(5) (a) Chowdhury, M. H.; Pond, J.; Gray, S. K.; Lakowicz, J. R. *J. Phys. Chem. C* **2008**, *112*, 11236. (b) Nallathamby, P. D.; Lee, K. J.; Xu, X. N. *ACS Nano* **2008**, *2*, 1371.

(6) Wiley, B.; Im, S.; Li, Z.; McLellan, J. M.; Siekkinen, A.; Xia, Y. *J. Phys. Chem. B* **2006**, *110*, 15666.

(7) (a) Haynes, C. L.; Van Duyne, R. P. *J. Phys. Chem. B* **2003**, *107*, 7426. (b) McFarland, A. D.; Young, M. A.; Dieringer, J. A.; Van Duyne, R. P. *J. Phys. Chem. B* **2005**, *109*, 11279.

(8) (a) Bharadwaj, P.; Anger, P.; Novotny, L. *Nanotechnology* **2007**, *18*, 044017. (b) Aslan, K.; Wu, M.; Lakowicz, J. R.; Geddes, C. D. *J. Am. Chem. Soc.* **2007**, *129*, 1524. (c) Zhang, J.; Malicka, J.; Gryczynski, I.; Lakowicz, J. R. *J. Phys. Chem. B* **2005**, *109*, 7643.

(9) Zhao, J.; Zhang, X.; Yonzon, C. R.; Haes, A. J.; Van Duyne, R. P. *Nanomedicine* **2006**, *1*, 219.

(10) (a) Atwater, H. A.; Maier, S.; Polman, A.; Dionne, J. A.; Sweatlock, L. *MRS Bull.* **2005**, *30*, 385. (b) Barnes, W. L.; Dereux, A.; Ebbesen, T. W. *Nature (London)* **2003**, *424*, 824. (c) Fang, N.; Lee, H.; Sun, C.; Zhang, X. *Science* **2005**, *308*, 534. (d) Zia, R.; Schuller, J. A.; Chandran, A.; Brongersma, M. L. *Mater. Today* **2006**, *9*, 20. (e) Hunter, E.; Fendler, J. H. *Adv. Mater.* **2004**, *16*, 1685. (f) Ozbay, E. *Science* **2006**, *311*, 189.

(11) (a) Jin, R. C.; Cao, Y. W.; Mirkin, C. A.; Kelly, K. L.; Schatz, G. C.; Zheng, J. G. *Science* **2001**, *294*, 1901. (b) Jin, R. C.; Cao, Y. W.; Hao, E. C.; Metraux, G. S.; Schatz, G. C.; Mirkin, C. A. *Nature (London)* **2003**, *425*, 487.

(12) (a) Lofton, C.; Sigmund, W. *Adv. Funct. Mater.* **2005**, *15*, 1197. (b) An, J.; Tang, B.; Ning, X.; Zhou, J.; Xu, S.; Zhao, B.; Xu, W.; Corredor, C.; Lombardi, J. R. *J. Phys. Chem. C* **2007**, *111*, 18055.

(13) (a) Hao, E.; Kelly, K. L.; Hupp, J. T.; Schatz, G. C. *J. Am. Chem. Soc.* **2002**, *124*, 15182. (b) Chen, S. H.; Fan, Z. Y.; Carroll, D. L. *J. Phys. Chem. B* **2002**, *106*, 10777. (c) Chen, Y. B.; Chen, L.; Wu, L. *Inorg. Chem.* **2005**, *44*, 9817. (d) Jiang, X.; Zeng, Q.; Yu, A. *Nanotechnology* **2006**, *17*, 4929.

(14) (a) Jana, N. R.; Gearheart, L.; Murphy, C. J. *Chem. Commun.* **2001**, 617. (b) Sun, Y.; Yin, Y.; Mayers, B. T.; Herricks, T.; Xia, Y. *Chem. Mater.* **2002**, *14*, 4736. (c) Sun, Y.; Xia, Y. *Adv. Mater.* **2002**, *14*, 833. (d) Caswell, K. K.; Bender, C. M.; Murphy, C. J. *Nano Lett.* **2003**, *3*, 667.

(15) (a) Nicewarner-Peña, S. R.; Freeman, R. G.; Reiss, B. D.; He, L.; Peña, D. J.; Walton, I. D.; Cromer, R.; Keating, C. D.; Natan, M. J. *Science* **2001**, *294*, 137. (b) Sun, Y. G.; Xia, Y. N. *Science* **2002**, *298*, 2176. (c) Kim, F.; Connor, S.; Song, H.; Kuykendall, T.; Yang, P. D. *Angew. Chem., Int. Ed.* **2004**, *43*, 3673. (d) Yu, D.; Yam, V. W. *J. Am. Chem. Soc.* **2004**, *126*, 13200. (e) Im, S. H.; Lee, Y. T.; Wiley, B.; Xia, Y. N. *Angew. Chem., Int. Ed.* **2005**, *44*, 2154.

(16) Wiley, B. J.; Xiong, Y.; Li, Z.; Yin, Y.; Xia, Y. *Nano Lett.* **2006**, *6*, 765.

(17) Zhou, J.; An, J.; Tang, B.; Xu, S.; Cao, Y.; Zhao, B.; Xu, W.; Chang, J.; Lombardi, J. R. *Langmuir* **2008**, *24*, 10407.

(18) (a) Sun, Y.; Mayers, B.; Xia, Y. *Nano Lett.* **2003**, *3*, 675. (b) Wiley, B. J.; Sun, Y.; Xia, Y. *Acc. Chem. Res.* **2007**, *40*, 1067.

(19) (a) Maillard, M.; Huang, P. R.; Brus, L. *Nano Lett.* **2003**, *3*, 1611. (b) Xue, C.; Mirkin, C. A. *Angew. Chem., Int. Ed.* **2007**, *46*, 2036. (c) Callegari, A.; Tonti, D.; Chergui, M. *Nano Lett.* **2003**, *3*, 1565. (d) Bastys, V.; Pastoriza-Santos, I.; Rodriguez-Gonzalez, B.; Vaisnoras, R.; Liz-Marzan, L. M. *Adv. Funct. Mater.* **2006**, *16*, 766. (e) Zheng, X.; Xu, W.; Corredor, C.; Xu, S.; An, J.; Zhao, B.; Lombardi, J. R. *J. Phys. Chem. C* **2007**, *111*, 14962.

(20) Xue, C.; Metraux, G. S.; Millstone, J. E.; Mirkin, C. A. *J. Am. Chem. Soc.* **2008**, *130*, 8337.

(21) Wu, X.; Redmond, P. L.; Liu, H.; Chen, Y.; Steigerwald, M.; Brus, L. *J. Am. Chem. Soc.* **2008**, *130*, 9500.

(22) (a) Kelly, K. L.; Coronado, E.; Zhao, L. L.; Schatz, G. C. *J. Phys. Chem. B* **2003**, *107*, 668. (b) Hao, E.; Schatz, G. C. *J. Chem. Phys.* **2004**, *120*, 357.

(23) Sun, Y. A.; Xia, Y. N. *Adv. Mater.* **2003**, *15*, 695.

(24) (a) Zhang, J.; Liu, H.; Zhan, P.; Wang, Z.; Ming, N. *Adv. Funct. Mater.* **2007**, *17*, 1558–1566. (b) Deivaraj, T. C.; Lala, N. L.; Lee, J. Y. *J. Colloid Interface Sci.* **2005**, *289*, 402–409.

JP810711A